Research Article

Ahmed Al Shouny*, Ragab Khalil, Abdullah Kamel, and Yehia Miky

Assessments of recent Global Geopotential Models based on GPS/levelling and gravity data along coastal zones of Egypt

https://doi.org/10.1515/geo-2022-0450
received August 12, 2022; accepted December 13, 2022

Abstract: The orthometric height has an essential role in a variety of civil engineering projects and it is defined as the length of the curved plumbline from a point (on the earth surface) to its intersection with the geoid surface. Leveling process is considered as the most accurate technique for obtaining these heights. However, regardless of its potentials, it is tedious, costly, and time consuming. Recently many organizations and research centers have developed multi Global Geopotential Models (GGMs) depending on several types of available gravity and height datasets to estimate orthometric heights from GNSS measurements. In this study, we present an evaluation and assessment of the accuracy of five of recent and popular GGM$_S$: XGM2016, XGM2019e, EIGEN-6C4, GO_CONS_GCF_2_TIM_R6e, and EGM2008 using actual 145 GNSS/leveling points and 96 terrestrial gravity points. The goal of this research is to find the best fit model along the study area located along the coastal zones of Egypt with distances of about 1,970 km for further determination of geoid modeling at regional scale. The selection of these areas basically was due to their developmental, urban, and economical importance and their continuous need for protection works to fight against the coastal erosion caused by climate change and global warming. The results indicated that for geoid undulation, GO_CONS_GCF_2_TIM_R6e model is the best fit GGM for the estimation of geoid model along Mediterranean Sea coastal line, while XGM2019e_2159 model is the best suitable for coastal line of the Red Sea. And regarding the gravity anomalies, the most reliable GGMs for this study area are XGM2019e_2159 and EIGEN-6C4 for Bouguer and free-air gravity anomaly, respectively.

Keywords: global geopotential models, geoid undulation, gravity anomaly, GNSS/leveling, terrestrial gravity data

1 Introduction

The actual height of any point on the physical surface of the Earth is called as orthometric height. This height is calculated as the distance along a plumbline (the gravity vector) from the point to the geoid. This orthometric height is essential for topographic maps, construction projects, plans, engineering designs, and many other civil engineering and geophysical applications. Spirit leveling process (with its different orders and standards) is considered as the most suitable and accurate technique for providing orthometric heights. The main concern is the time needed for performing this technique, which drive up work's cost, and the logistical difficulties such as large areas and obstructions. So, one of the most challenging tasks for surveyors and geodesists is to investigate the capability of using any alternative techniques for estimating orthometric heights.

Recently, with the widespread and extensive utilization of modern positioning satellite systems and their newly developed techniques and applications, the 3-dimensional coordinates: latitude, longitude, and ellipsoidal height (ϕ, λ, and h) could routinely be determined with high accuracy. This ellipsoidal height can be transformed into orthometric heights using a suitable precise geoid model, as an alternative method to leveling. The geoid model is classified into three types according to the available data used in modeling

* **Corresponding author: Ahmed Al Shouny,** Department of Geomatics, King Abdulaziz University, Jeddah, Saudi Arabia; Survey Research Institute, National Water Research Center, Giza, Egypt, e-mail: ametaowa@kau.edu.sa
Ragab Khalil: Civil Engineering Department, Faculty of Engineering, Assiut University, Assiut, Egypt; Civil Engineering Department, Faculty of Engineering and IT, Onaizah Colleges, Qassim, KSA, e-mail: ragabkhalil@oc.edu.sa
Abdullah Kamel: Department of Geomatics, King Abdulaziz University, Jeddah, Saudi Arabia, e-mail: amakamel@kau.edu.sa
Yehia Miky: Department of Geomatics, King Abdulaziz University, Jeddah, Saudi Arabia; Faculty of Engineering, Aswan University, Aswan, Egypt, e-mail: yhhassan@kau.edu.sa
ORCID: Ahmed Al Shouny 0000-0003-0427-4079; Yehia Miky 0000-0003-3544-0228

the geoid. The geometric models use GPS and leveling data, while the gravimetric models use different types of gravity data such as airborne gravimetry, terrestrial gravimetry, and satellite gravimetry. When using both types of these data, a combined geoid model is produced. Also, this geoid model can be classified into local or global models depending on the covered area and the available data along this area. Local geoid models are suitable for small areas to achieve a high precision taking into consideration some factors as accuracy of the available data and its separated distances, and the interpolation method used [1]. For large areas, global models are preferred, so, many organizations and research centers have developed multi Global Geopotential Models (GGMs) depending on several types of available gravity and height datasets. Each of these GGMs has its own advantages, and their accuracy differs according to the region. Therefore, evaluation of the performance of these GGMs is essential in the selection of the optimal model for each area.

Many studies discuss the performance of several recent GGMs over different regions. And due to the vital location of Egypt region and its important area, several researchers studied different GGMs along different areas of Egypt. The major goal of these studies is to evaluate and compare the results of the recent GGMs to determine the best fit model along the investigated area [2–5]. Many other studies showed interests on developing an accurate geoid model by enhancing or merging data of different models [6–8]. All these studies differ due to the available data, the selected GGMs, the spherical harmonic coefficient variation, and the investigated study area [5].

In this study, five of the recent and common GGMs are represented, evaluated, compared, and analyzed in order to determine the best fit GGMs along the study area. We selected these 5 GGMs from all available GGMs due to their acceptable results in the recent similar studies and also, we chose them from models with different data types and sources. This area is located in Egypt, it is divided into two separated zones along the coastal lines of Mediterranean and Red Sea. These seaside zones comprise an especially significant region, economically, industrially, socially, and culturally [9]. These important coastal regions need to be protected continuously using protection works to fight erosion caused by the relative rise in sea level due to the consequences of global warming [10–12]. And also there are many important urban, tourism, and development projects that are being held continuously along these coastal areas. So, it is important to have an accurate geoid model to estimate the required orthometric heights in acceptable accuracy and also to have a suitable gravimetric model to conduct geodynamic and geophysical explorations as crustal movements. Thus, the selected five GGMs called XGM2019e, XGM2016, EGM2008, EIGEN-6C4, and GO_CONS_TIM_R6e are evaluated and compared along these areas. The comparison is based on (free-air and Bouguer) gravity anomalies, geoid undulation estimated from these models with datasets containing real GPS/leveling and gravity data points available along the study area. This study is organized as follows: first GGMs are presented, then the assessment criteria was discussed. Second, the study area and available data are introduced. Third, the results of the study are presented and discussed. Finally, conclusion for this work is demonstrated with respect to some important perspectives for future work.

2 GGMs

Geoid can be defined as an equipotential surface of gravity potential that corresponds to the continuous, worldwide sea level. It serves as the most accurate and ideal height reference surface and is the physical representation of the Earth [13,14]. The accurate determination of height related to geoid surface, orthometric height, relies on how accurate the available data of gravity is. So, an accurate definition of the global gravity field of the Earth is one of the main important objectives of geodesy. Nowadays, thanks to the derived precise measurements from satellite, which is a result of advancing technology, we can determine better spatial and temporal resolutions of global gravity field of the Earth and its variation compared to the first-generation of global gravity field models from 1960s to 1990s. Recently, due to the modern missions of satellite gravity, several types of GGMs are freely available, particularly the gravity field and steady state ocean circulation explorer (GOCE) and also the gravity recovery and climate experiment (GRACE) [15]. Several organizations and research centers have produced more than 175 GGMs [16]. Users can download these models using a free service developed by the International Center for Global Earth Models (ICGEM) [17].

The GGMs may be outlined as a mathematical model in a spectral domain for the calculation of gravitational potential using spherical harmonic expansion. GGMs ordinarily outline the value of the gravitational potential of the Earth by using fully normalized Stokes' coefficients for each degree n and order m (C_{nm} and S_{nm}). Based on these available coefficients of every degree and order, Earth's gravity potential functionals can be extracted [18,19]. These GGMs provide several information about the Earth such as geoid undulation, normal gravity, gravity anomaly, vertical deflection, and gravity disturbance. GGMs are categorized into

three major types called satellite-only, combined, and tailored models [19,20].

1. Satellite-only models are generated from the observations of artificial Earth satellite. Due to several issues, such as a lack of continuous tracking data from the existing stations, challenges modeling non-gravitational, third body perturbations, insufficient sampling of the global gravitational field, weakening of the gravitational field with altitude, and precession of the Earth-based range measurements to the satellites, these models have some precision limitations. Due to the recent dedicated satellite gravimetric missions such as CHAMP, GRACE, GOCE, and LAGEOS, many of these limitations were minimized significantly [21–24].
2. Combined models are computed using the combination of several data sources including terrestrial gravity observations, land and ship gravity data, recently airborne gravity data, and marine gravity anomalies derived from satellite altimetry in addition to satellite data. Therefore, these combined models allow to increase the degree of spherical harmonics which improves the quality of results obtained using these models if compared with satellite-only models. However, these models also have limitations in precision similar to satellite-only models caused by the same deficiencies in addition to the other errors caused by the newly used data [22,23,25].
3. Tailored models are derived as a result of adjusting and enhancing the coefficients of the spherical harmonic of GGMs for satellite-only or combined models to higher degree by adding new gravity dataset that may not necessarily have been used before. These models' primary goal is to increase the model degree. Because spurious effects can occur in locations where there are no data available, it is important to note that tailored GGMs only apply over the area in which the tailoring was applied. EGTGM2014, EG1GOC5s, and EGTM0818 are examples of tailored geopotential models [22,23].

In this research, five of the recent and popularly used GGMs have been represented, evaluated, and compared using the maximum available degree and order of each of the selected models. A brief definition of these models are represented her and also Table 1 illustrates a comparison between these models.

1. Earth geopotential model (EGM, 2008): it is the most recent and popular EGM as we are waiting for the release of the integrated Earth gravitational model 2020 (EGM, 2020). EGM2008 has been produced and publicly released for users by the US National geospatial-intelligence agency (NGA). It can be defined as a model for calculating the spherical harmonic of the Earth's gravitational potential. EGM2008 is complete to the degree and order 2,159, and contains additional coefficients extending to the degree 2,190 and order 2,159 [4,24].
2. Experimental gravity field model (XGM, 2016): NGA developed and released the XGM2016 on 22nd May, 2017 as a preliminary result of the upcoming EGM2020. XGM2016 extends to spherical harmonic degree of 719, that is the highest resolution supported by its $15' \times 15'$ terrestrial grid for XGM2016, a major focus is going to be the best combination of the new terrestrial data with the most recent satellite gravity data [3,26].
3. XGM2019e: it is one of the recent GGM, it has been released on 25th September, 2019 by the Technical University of Munich and it is available in three different expansions. This model contains two sources of data, GOCO06s satellite data within the longer wavelength area and terrestrial data with shorter wavelengths over both land and ocean areas. This mixture of the terrestrial observations with the satellite data is performed by using full normal equations up to d/o 719 (15′). XGM2019e is published in three versions truncated to d/o 2,160, 5,540, and 760 [23].
4. European improved gravity model of the Earth (EIGEN-6C4): it is a static global combined gravity field model up to

Table 1: Comparison between the selected GGMs evaluated in this study

No.	Model	Year	Degree	Data	Reference
1	EGM2008	2008	2,190; 5,540; 760	S (GRACE), G, A	[34]
2	XGM2016	2017	719	A, G, S(GOCO05s)	[35,36]
3	XGM2019e	2019	760	A, G, S(GOCO06s), T	[37]
4	EIGEN-6C4	2014	2,190	S (GOCO, GRACE, LAGEOS), G, A	[38]
5	GO_CONS TIM_R6E	2019	300	G(polar), S(GOCE)	[29,37]

Note: S is the satellite data (e.g., GOCE, GRACE, and LAGEOS), **G** is the terrestrial gravity data, **A** is the altimetry data, and **T** is for the topography.

degree and order of 2,190. It was produced in 2nd December of 2014 by the collaboration between Groupe de Recherche de Géodésie Spatiale (Space geodesy research group; GRGS), Toulouse and GeoForschungsZentrum (Geo-research center) (GFZ), Potsdam [24,27,28].

5. GO_CONS_GCF_2_TIM_R6e: The sixth release of the GOCE gravity field model, TIM R6e, was available in July 2019 using a time-wise approach. The extraterrestrial gravity field observations across GOCE's polar gap zones are regarded as an extended version of the satellite-only global gravity field model TIM R6 [29]. The data from the PolarGap campaign [30] supplemented by the AntGG gravity data compilation [31] over the southern polar gap (>83°S) and the ArcGP data [32] over the northern polar gap (>83°N) make up the included terrestrial information [33].

3 Assessment criteria

In order to validate the above mentioned GGMs, their estimated values (geoid undulation and gravity anomaly) have to be compared with corresponding accurate values calculated using available terrestrial data. Geoid undulation is defined as the difference between the ellipsoid height (h), related to ellipsoid surface, measured by GPS measurements and the orthometric height (H), related to M.S.L, estimated using Leveling observations, as shown in Figure 1 and calculated using equation (1) [9]. The geoid undulation value calculated using the available GNSS/leveling points, ($N_{\mathrm{GNSS/Leveling}}$) is compared with the corresponding GGMs derived value of undulation (N_{GGMs}) which is calculated using equation (2) [39].

$$N_{\mathrm{GPS/levelling.}} = h - H, \tag{1}$$

$$N_{GM} = \frac{GM}{\gamma r}\sum_{n=0}^{n_{\max}}\left(\frac{R}{r}\right)^{n}\sum_{m=0}^{n}P_{nm}(\cos\theta)(c_{nm}\cos m\lambda + s_{nm}\sin m\lambda), \tag{2}$$

where θ, λ, and r are the point's co-latitude, longitude, and geocentric radius, respectively; R is the reference ellipsoid's major axis radius; GM is created by multiplying the Earth's mass by the gravitational constant; γ is the reference ellipsoid's mean gravity; C_{nm} and S_{nm} are the series development Stokes coefficients; P_{nm} n-degree and m-order representation of the linked Legendre functions.

The normal gravity field is the gravitational field of a reference ellipsoid of rotation that closely approximates the real Earth. The gravity anomalies (Δg), also used in the evaluation of GGMs, is defined as the difference between the true gravity (g) measured on the physical surface (geoid) of the Earth using means of the acceleration of the free fall and the corresponding normal gravity value (y_o) derived by a gravity field model of the reference ellipsoid and it can be calculated using equations (3)–(5) [40–42] as follows:

$$\Delta g = g - y_o. \tag{3}$$

There are two values of gravity anomalies called free-air (Δg_{FA}) and Bouguer (Δg_{SB}) anomalies which are given as follows:

$$\Delta g_{\mathrm{FA}} = g + F - y_o, \tag{4}$$

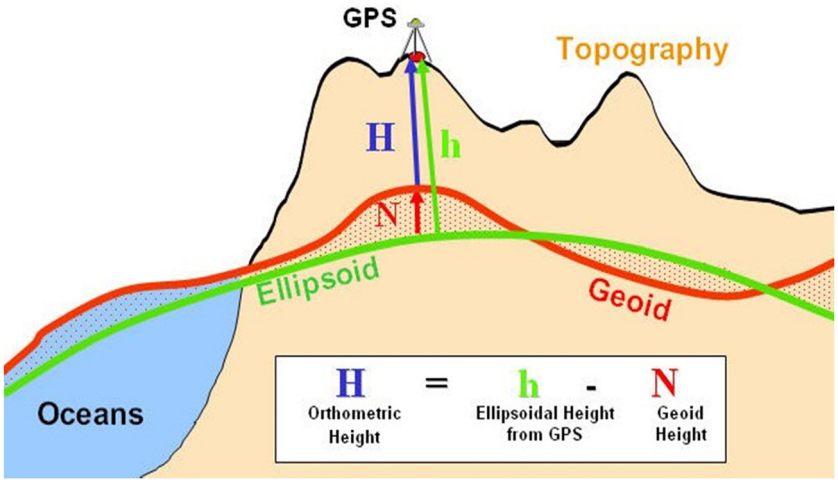

Figure 1: The relationship between ellipsoidal, orthometric, and geoid height [9].

where F is the correction of the free-air in mGal = 0.3086 H (approximation); H is the geoid height in m. And,

$$\Delta g_{SB} = g + F - B - \quad y_o, \tag{5}$$

where SB is the simple Bouguer gravity anomaly; B is the simple Bouguer correction = −0.1119 H (approximation).

The gravity anomaly derived from GGMs up to spherical harmonic degree n_{max} can be calculated by equation (6) [2]:

$$\Delta g_{GM} = \frac{GM}{r^2}\sum_{n=0}^{n_{max}}\left(\frac{R}{r}\right)^n (n-1) \times \sum_{m=0}^{n} P_{nm}(\cos\theta)(c_{nm}\cos m\lambda + s_{nm}\sin m\lambda), \tag{6}$$

where the components of equation (6) are previously presented in equation (2).

It should be noted that during geoid model's computation, we take into consideration three permanent tide systems. In these three systems, the geoid can be summarized as follows:

- Tide-free (or nontidal): This geoid is taken into account for a tide-free Earth with no residual influences from the sun and moon.
- Mean-tide: This geoid is taken into account when the sun and moon are present (or, equivalently, if no permanent tidal effects are removed).
- Zero-tide: This geoid is taken into consideration if the long-term direct impacts of the sun and moon are eliminated but the indirect effect component associated with the Earth's elastic deformation is retained [17].

4 Study area and available terrestrial data

The study area is located in Egypt, and it was categorized into two main regions; A and B along the coastal zone lines of Egypt. The selection of these areas basically was due to their continuous need for protection works to fight against the coastal erosion caused by the climate change and global warming. Area A is located at the northern zone of Egypt along the Mediterranean Sea, starting from El Alamein city west and extends to Al Areesh governorate east, with a longitudinal distance of about 520 km. The second area B is located at the eastern zone of Egypt along both the sides of Red Sea Suez Gulf and extending to Aqaba Gulf, with a longitudinal distance of about 1,450 km. Figure 2 shows the flowchart of the study methodology.

The evaluation of the investigated GGM_S in this research was performed using two categories of terrestrial dataset. This dataset contains 145 GNSS/leveling points and 96 land gravity points distributed along the study area. Figure 3 represents the study area and the locations of the available data along this area. GNSS/leveling points were established, observed, and adjusted by Survey Research Institute (SRI) in cooperation with the Egyptian Coastal Protection Agency in several projects and reports [43]. These points were established using specific standards to ensure their sustainability for any future use of different surveying works surrounding these regions as shown in Figure 4a. All these points' orthometric heights were measured using precise spirit leveling process to be calculated to achieve the first-order class leveling standards [44].

Observations were performed using Wild N3 optical level with micrometer accuracy of 0.1 mm, using Invar Staff, as shown in Figure 5a, to ensure achieving the required standards. All points were connected to the nearest known first-order benchmarks established by the Egyptian Survey Authority (ESA) with a closed leveling loop that achieved a maximum allowable mis-closures between the two leveling ways of $\pm 5\sqrt{L}$ in mm, where L is the route length of the leveling (one way) in kilometers. The measurements followed the reading sequences of "backsight – foresight – foresight backsight" and then "foresight – backsight – backsight – foresight" to have redundant observations to check measurements and eliminate blunder errors. The average mis-closure for all points is about $\pm 4.25\sqrt{L}$ which means that it achieves the required accuracy. Also, the orthometric correction was applied to the leveling results to increase the precision of the obtained orthometric heights of points.

Also, GPS measurements were carried out for all these points for a long time at different epochs using static observing technique to determine their precise 3-Dimensional geographic coordinates (latitude, longitude, and ellipsoidal height). The observations were divided into multi separated networks, each one containing the established points and the available ESA first-order triangulation stations shown in Figure 4b in the surrounding area. These networks were designed as an over-constrained geodetic network [45] to detect and isolate blunders and systematic errors from measurements and to guarantee the consistency and accuracy of the estimated coordinates of these network points. Dual frequency GPS receiver model of Trimble 5700 shown in Figure 5b was utilized during the observation sessions to eliminate most of the ionospheric effects.

The data processing was performed with a confidence level of 95% using precise ephemeris to increase the accuracy of the estimated coordinates, thanks to Trimble Business Center software. Also, an adjustment process was performed

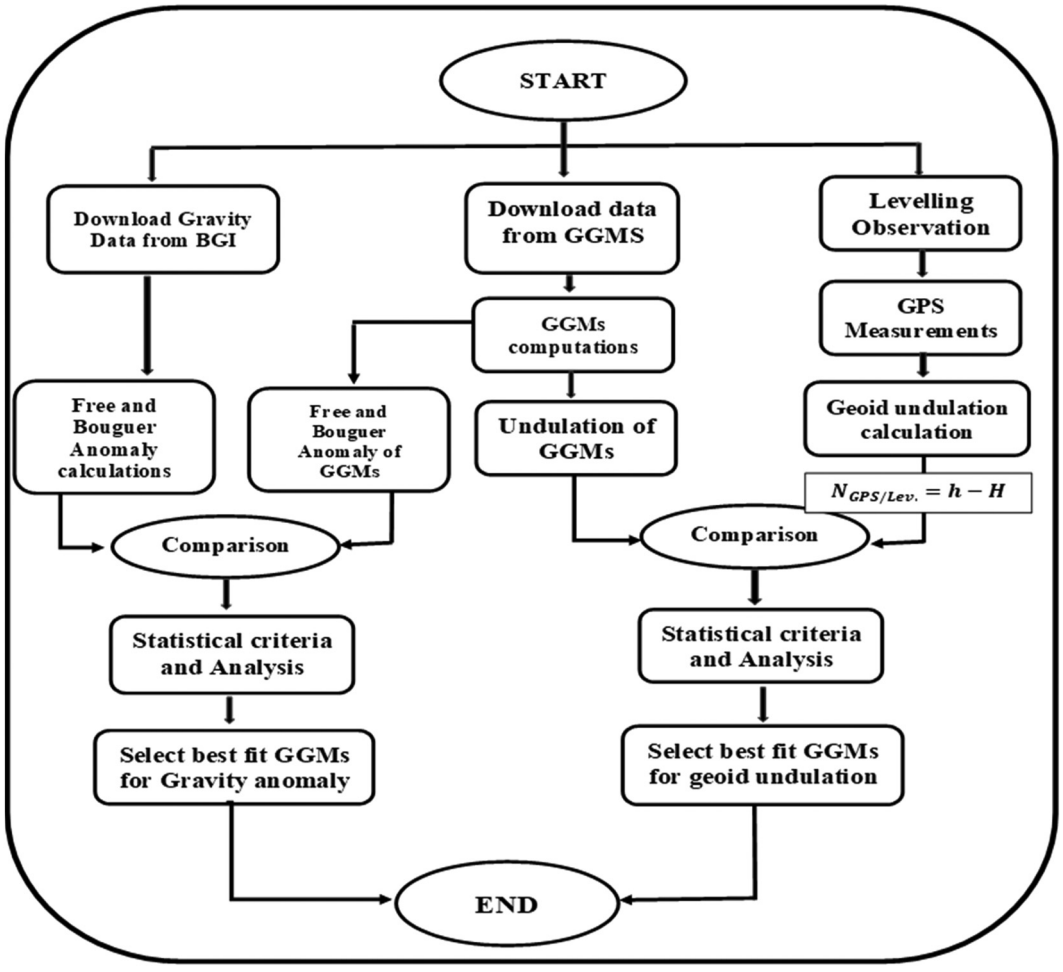

Figure 2: Flowchart of the study methodology.

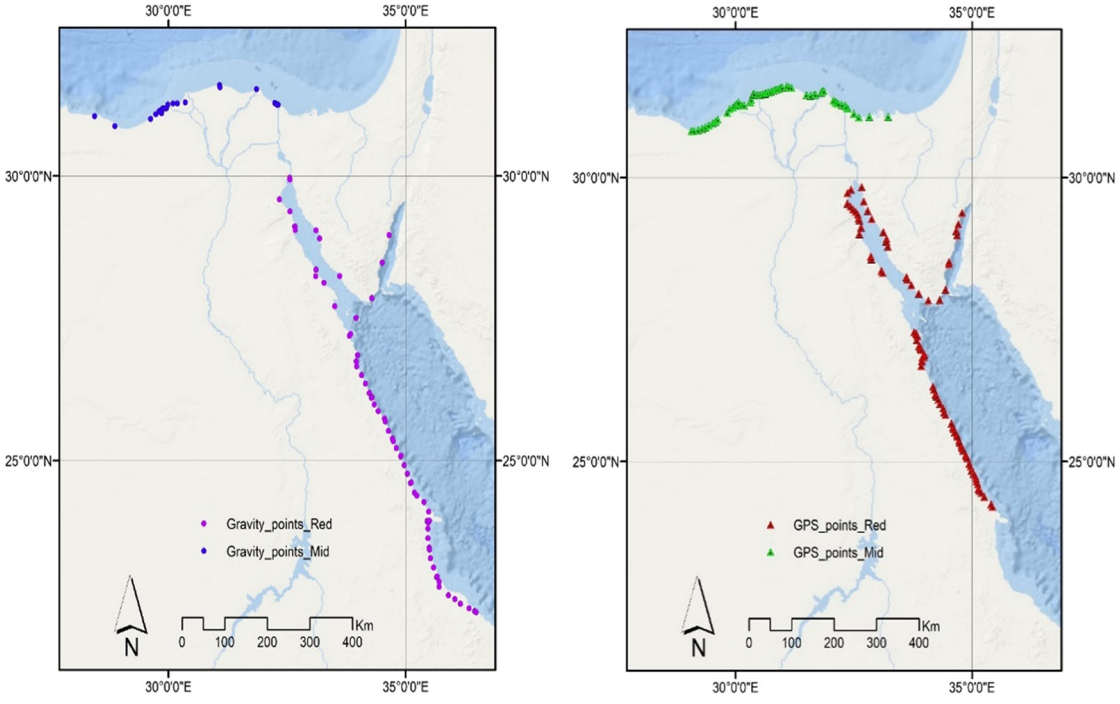

Figure 3: The study area and the locations of both types of available data.

(a) (b)

Figure 4: Network point and ESA first-order station. (a) Established control point. (b) ESA station.

(a) (b)

Figure 5: Instruments used in the surveying works. (a) Optical level instrument. (b) Trimble 5700 GPS instrument.

to decrease errors and determine the accurate points' coordinate values achieving the required precision of ±"2 cm + 1 PPM" (parts per million) for horizontal positions and ±"5 cm +1 PPM" for vertical ellipsoid height. The horizontal precision for points ranged from 0.003 to 0.020 m, while the vertical precision ranged from 0.005 to 0.045 m.

The land gravity data used in this study were obtained from the international gravimetric bureau (BGI) in France

[46]. These gravity data are in the geodetic reference system 1980, and their measured gravity values have been connected to International Gravity Standardization Net system adopted in 1971 [47]. The accuracy of the used land gravity values is about 0.25–0.75 mGal [42].

To assess the selected GGMs in this research as discussed in assessment criteria section, two values (geoid undulation and gravity anomaly), which are calculated by GGMs, were compared using their corresponding accurate values estimated from available terrestrial data. Geoid undulation at the locations of the available GNSS/leveling points was calculated using the selected five GGMs. The calculation service is available on ICGEM website using user-defined points service, and for models, there are several degrees and we selected the maximum available degree. Then the differences (residuals) between the values derived using each model and measured using GNSS/leveling points, from equation (1) were calculated. These residual values express the achievable quality of each GGMs. Some statistical criteria were calculated and then compared for these obtained residual values. These criteria are maximum, minimum, median, standard deviations (SDs), and root mean square error (RMSE). These statistical results are represented for both the zones, area (A) and (B) in Tables (2 and 3) and are shown in Figures 6 and 7. To illustrate the consistency of these obtained results, box plots were represented to graphically figure out the variation between these investigated GGMs as shown in Figures 8 and 9.

Also, the gravity anomalies values estimated from GGMs were compared with those measured via the available land gravity data used in this research. This comparative evaluation of both the derived (free-air and (simple) Bouguer) gravity anomalies was performed using the residuals between the derived values of GGMs and the corresponding values measured using terrestrial gravity data. The same univariate descriptive statistics, used in geoid undulation comparisons, were used here for both free-air and Bouguer gravity anomalies as represented in Tables 4 and 5, and shown in Figures 10 and 11. Box plots of these estimated residual values for free-air and Bouguer gravity anomalies are shown in Figures 12 and 13. Also, residual maps for both the free-air and Bouguer gravity anomaly along the study area were drawn using the ArcGIS software as shown in Figures 14–18.

5 Discussion of the results

The objective of this study is to evaluate the selected GGMs accuracy along the study area through the geoid undulation values as well as the gravity anomaly. So, the geoid undulation values were first calculated from GNSS/leveling points in both the regions A and B, where the values ranged from 10.973 to 17.756 m. Then the geoid heights were extracted from the five GGMs, with the maximum available degree. An interpolation was made to obtain the geoid height information of GNSS/leveling locations from GGMs. The geoid heights determined from the five GGMs are ranged between 10.562 and 18.875 m.

Table 2: Models' statistics of Mediterranean Sea zone points' undulation variations (m)

Statistics	EGM2008	XGM2019e_2159	XGM2016	EIGEN-6C4	GO_CONS_GCF_2_TIM_R6e
Maximum	1.171	1.051	1.008	1.022	0.897
Minimum	0.354	0.471	0.448	0.420	0.349
Median	0.823	0.780	0.814	0.794	0.686
Standard deviations	0.218	0.129	0.141	0.143	0.117
RMSE	0.830	0.791	0.788	0.787	0.670

Table 3: Models' statistics of Red Sea zone points' estimated undulation variations (m)

Statistics	EGM2008	XGM2019e_2159	XGM2016	EIGEN-6C4	GO_CONS_GCF_2_TIM_R6e
Maximum	1.088	0.592	0.650	1.034	1.571
Minimum	−1.493	−0.676	−0.607	−0.783	−0.772
Median	0.231	0.011	−0.050	−0.021	0.318
Standard deviations	0.564	0.305	0.348	0.397	0.470
RMSE	0.598	0.303	0.347	0.395	0.559

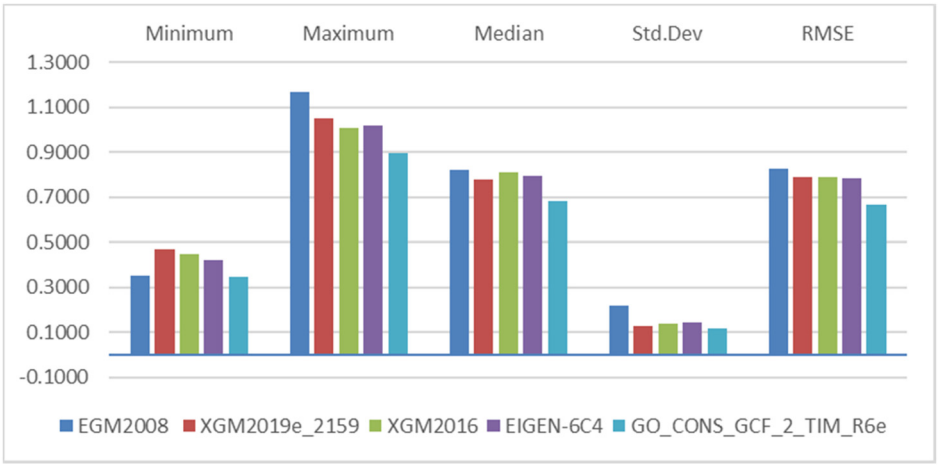

Figure 6: Models' statistics of Mediterranean Sea zone points' undulations deviations.

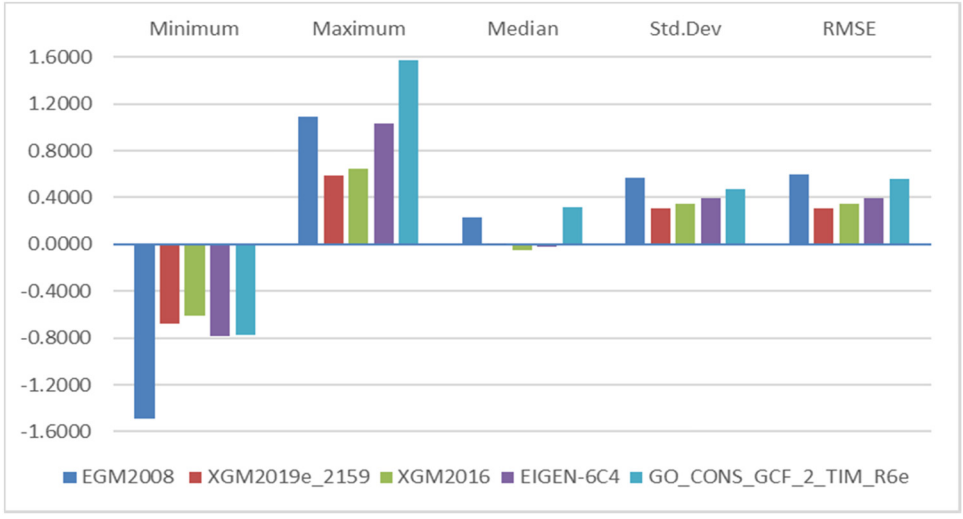

Figure 7: Models' statistics of Red Sea zone points' undulations deviations.

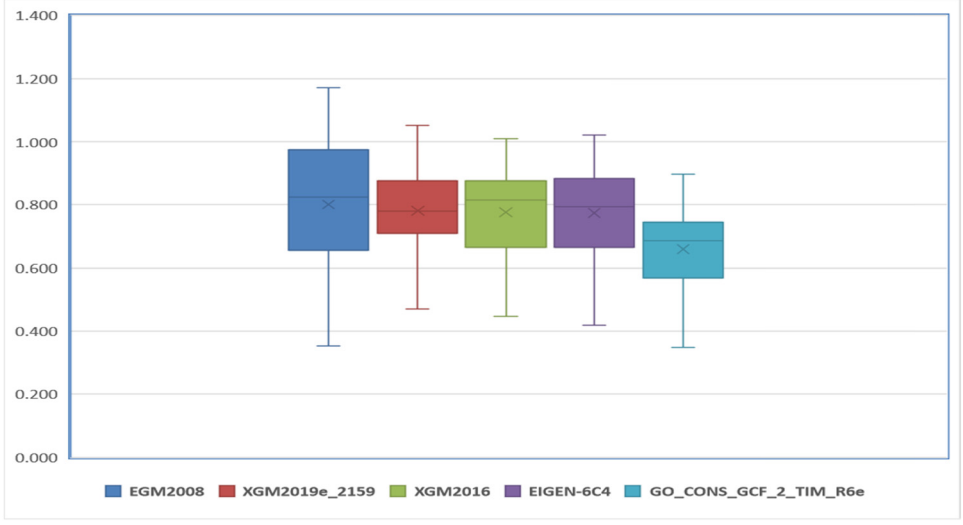

Figure 8: Box plot of geoid undulation deviations along the Mediterranean Sea zone.

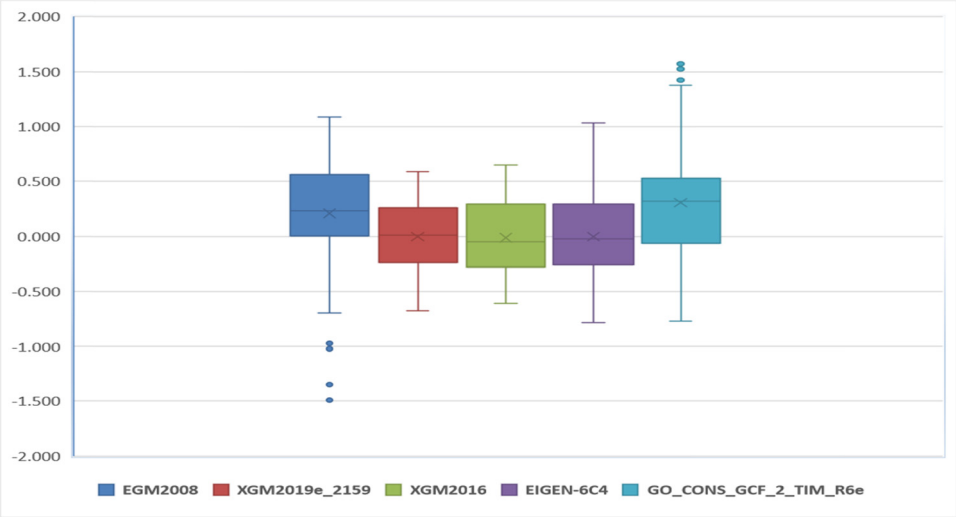

Figure 9: Box plot of geoid undulation deviations along the Red Sea zone.

Table 4: Models' statistics for Bouguer gravity anomalies deviations in the study area (in mGal)

Statistics	EGM2008 MODEL	XGM2019e_2159	XGM2016	EIGEN-6C4	GO_CONS_GCF_2_TIM_R6e
Maximum	51.088	44.475	56.137	36.487	57.160
Minimum	−26.031	−40.636	−28.436	−36.767	−29.059
Median	1.908	0.317	0.206	1.578	−0.322
standard deviations	12.227	12.948	12.871	12.386	15.628
RMSE	12.563	12.890	12.820	12.373	15.554

Table 5: Models' statistics for free-air gravity anomalies deviations in study area (in mGal)

Statistics	EGM2008	XGM2019e_2159	XGM2016	EIGEN-6C4	GO_CONS_GCF_2_TIM_R6e
Maximum	51.878	52.451	39.711	40.951	93.101
Minimum	−26.429	−41.038	−44.798	−37.184	−42.437
Median	1.500	0.315	−0.502	−0.078	2.761
SD	13.055	13.183	14.647	12.720	21.888
RMSE	13.326	13.119	14.574	12.691	22.349

Depending on the statistics shown in Tables 2 and 3, the estimated geoid undulations calculated from the five GGMs are compared with undulation values estimated using the GNSS/leveling for the 145 points established along the coastal lines of Egypt; regions A and B had a maximum difference of 1.1707 m, in EGM2008 for region A, and 1.5710 m, in GO_CONS_GCF_2_TIM_R6e for region B. As shown in Table 2, RMSE of the geoid undulations residuals values estimated for the 145 points by subtraction geoid undulations values calculated from GNSS/leveling data and values that obtained from the 5 GGMs indicated that EGM2008 has the biggest RMSE of all models. The minimum values of the RMSE of the residual surface were 0.6697 m from GO_CONS_GCF_2_TIM_R6e and 0.3033 m from XGM2019e for regions A and B, respectively.

From the Box plots, shown in Figures 8 and 9, for the residuals between the geoid undulations calculated from the GNSS/leveling and those derived from the five GGMs for region A, GO_CONS_GCF_2_TIM_R6e model recorded the lowest median value (0.6858 m), followed by XGM2019e, EIGEN-6C4, and then XGM2016, where the EGM2008 had recorded the highest median value of 0.8234 m. Regarding the range, EGM2008 recorded the largest value (0.8168 m) followed by EIGEN-6C4 and then XGM2019e and XGM2016,

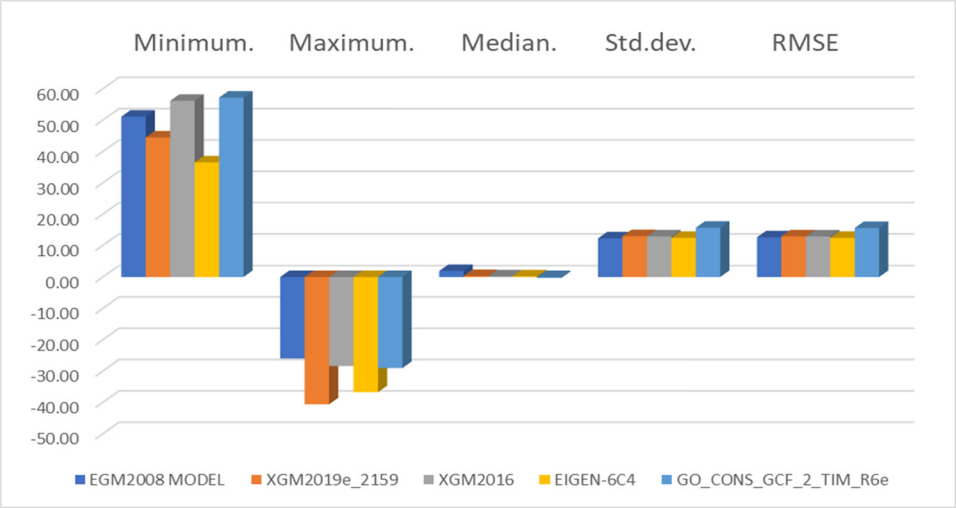

Figure 10: Models' statistics for Bouguer gravity anomalies deviations in the study area.

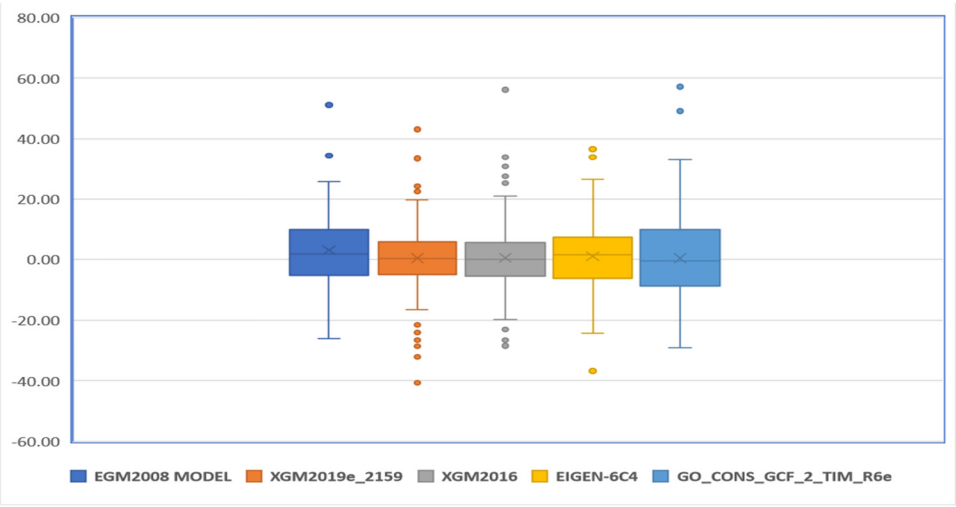

Figure 11: Box plot of study area points' Bouguer gravity anomalies deviations for the five models.

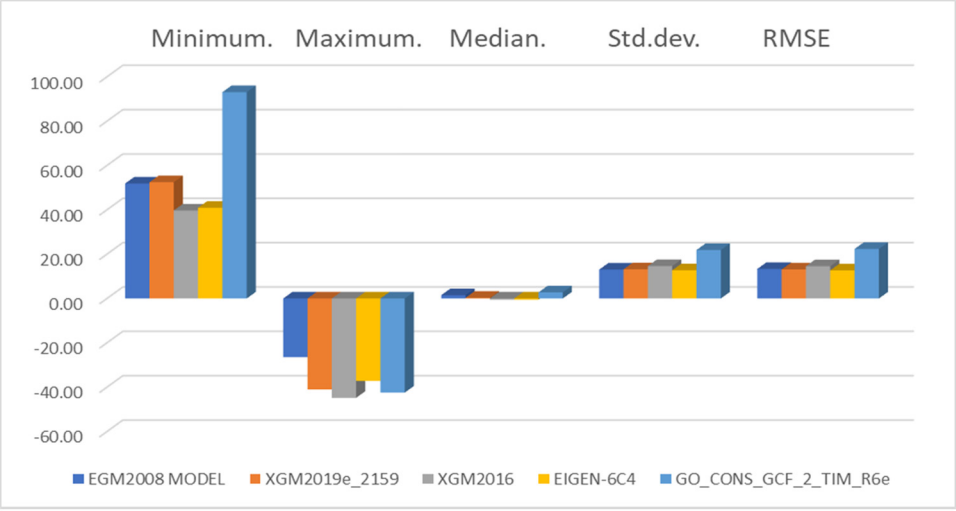

Figure 12: Models' statistics for free-gravity anomalies deviations in the study area.

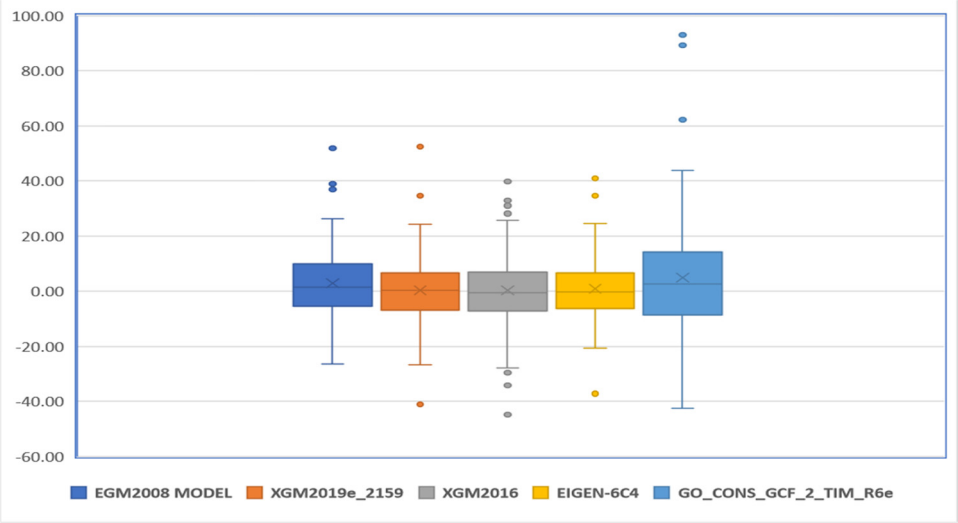

Figure 13: Box plot of study area points' free-air gravity anomalies deviations for the five models.

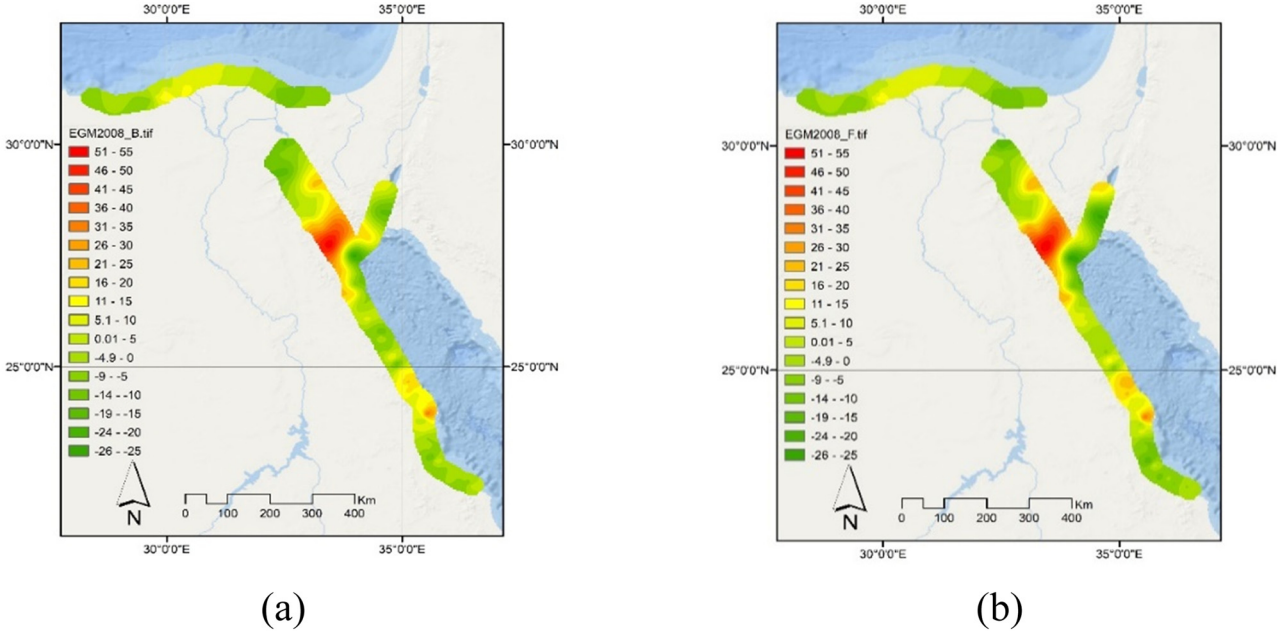

Figure 14: EGM2008 residual map of gravity anomaly (in mGal): (a) Bouguer and (b) Free-air.

where the smallest value of range was recorded in GO_CONS_GCF_2_TIM_R6e. It was 0.5481 m. It is also noticed that, among all Box plots, the one for XGM2019e is not skewed, while box plots for other models appear to be skewed left. In region B, XGM2019e model had recorded the lowest absolute median value (0.011 m) followed by EIGEN-6C4, XGM2016, and then EGM2008, where GO_CONS_GCF_2_TIM_R6e model has recorded the highest absolute median value (0.3180 m). Also, as in region A, the range of EGM2008 was the largest, the value was 2.581 m followed by GO_CONS_GCF_2_TIM_R6e model and then EIGEN-6C4 and XGM2019e. XGM2016 model had recorded the smallest range value of 1.257 m. Box plots for XGM2019e, GO_CONS_GCF_2_TIM_R6e, and EGM2008 are not skewed, while box plots for XGM2016 and EIGEN-6C4 models are skewed to the left. As a result, we concluded that among the five GGMs examined in this study, the GO_CONS_GCF_2_TIM_R6e model is more suitable GGM for determining a suitable geoid model in region A, along the Mediterranean Sea, while

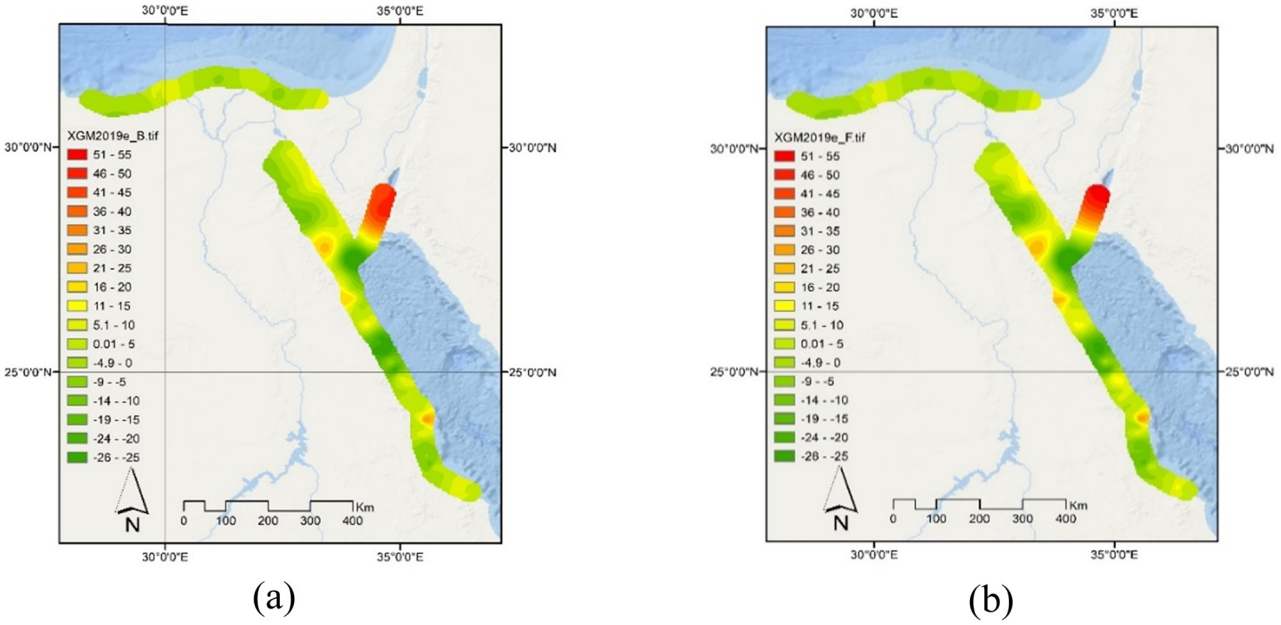

Figure 15: XGM2019e residual map of gravity anomaly (in mGal): (a) Bouguer and (b) Free-air.

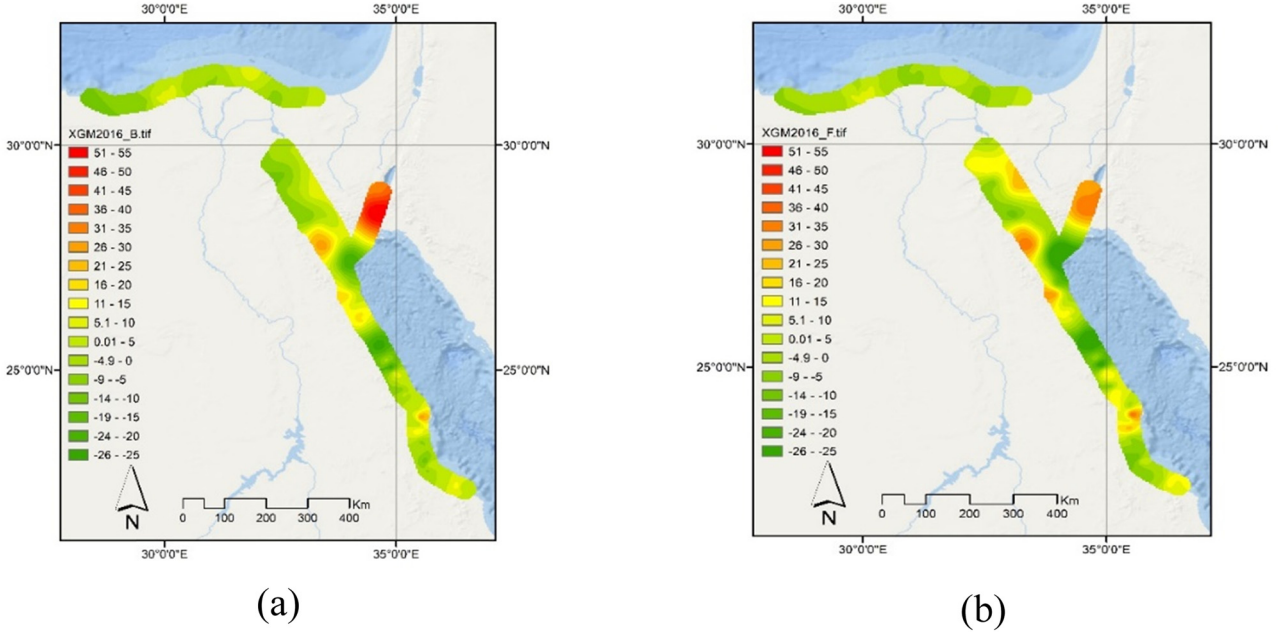

Figure 16: XGM2016 residual map of gravity anomaly (in mGal): (a) Bouguer and (b) Free-air.

XGM2019e model is more suitable for region B, along the Red Sea.

Regarding both the Bouguer and free-air gravity anomalies, deviations statistics for the five GGMs are compared with those derived from the land gravity measurements as shown in Tables 4 and 5, respectively. The maximum deviation range of Bouguer gravity anomaly was recorded for GO_CONS_GCF_2_TIM_R6e model, it was 86.219 mGal (the maximum was 57.160 mGal and the minimum was −29.059 mGal), followed by XGM2019e_2159, XGM2016, and EGM2008. Whereas the minimum deviation range was found in EIGEN-6C4 model, it was 73.254 mGal (the maximum was 36.487 mGal and the minimum was −36.767 mGal). The same performance was noticed

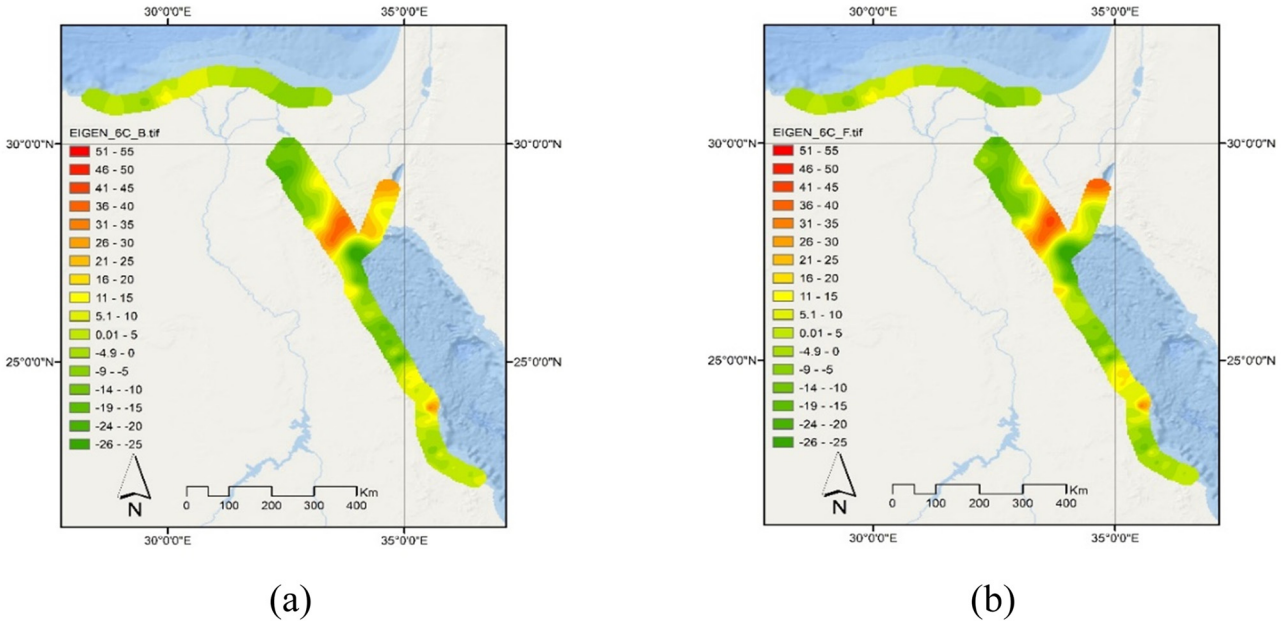

Figure 17: EIGEN-6C4 residual map of gravity anomaly (in mGal): (a) Bouguer and (b) Free-air.

f-

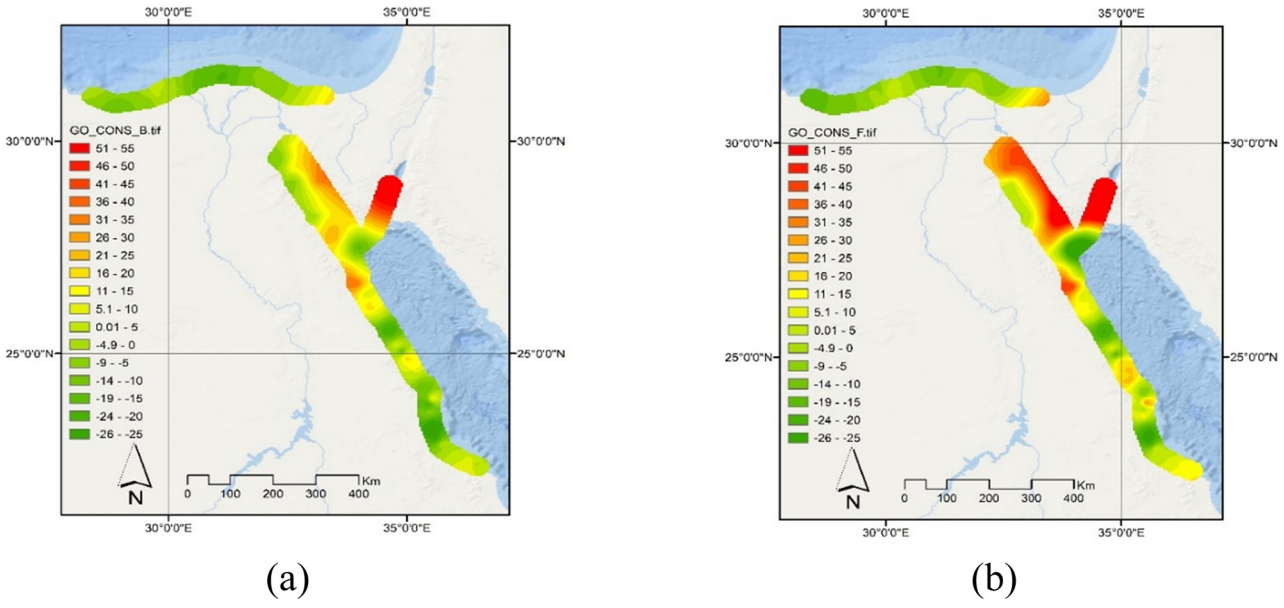

Figure 18: GO_CONS_GCF_2_TIM_R6e residual map of gravity anomaly (in mGal): (a) Bouguer and (b) Free-air.

or free-air anomalies, the maximum deviation range was in GO_CONS_GCF_2_TIM_R6e model where the range was 135.538 mGal (93.101 as a maximum and −42.437 as a minimum), followed by XGM2019e_2159, XGM2016, and EGM2008. Also, EIGEN-6C4 model recorded the minimum deviation range of 78.136 mGal, the values were 40.951 and −37.184 mGal for the maximum and minimum, respectively.

Based on the results, regardless of GO_CONS_GCF_2_TIM_R6e model having recorded the highest SD among all the tested models, there is no big difference on the values for the rest of the models, their performances are similar. The maximum values of the residuals RMSE, when comparing the land gravity measurements with those extracted from the five GGMs, were from GO_CONS_GCF_2_TIM_R6e model in both the Bouguer and free-air gravity.

They were 15.554 and 22.349 mGal, respectively. The minimum values were from EIGEN-6C4 model, they were 12.373 and 12.691 mGal for both Bouguer and free-air gravity, respectively.

As can be seen in Figures 10 and 11, for the residuals between the gravity anomaly derived from the land locations measurements and those derived from the five GGMs, XGM2016 model had the lowest absolute median of about 0.206 mGal followed by XGM2019e, GO_CONS_GCF_2_TIM_R6e, and EIGEN-6C4 in a sequence, where the highest median was recorded in EGM2008 which was 1.908 mGal for the Bouguer gravity anomalies. For the free-air gravity anomalies also, XGM2016 model had the lowest absolute median of about 0.326 mGal followed by XGM2019e, and EIGEN-6C4, and EGM2008 in a sequence, where the highest median was recorded in GO_CONS_GCF_2_TIM_R6e model, it was 5.039 mGal. Box plots of all models seemed to be not skewed, but many outliers appeared spatially when using XGM2016 model. Despite the results obtained from the GO_CONS_GCF_2_TIM_R6e model, one can conclude that all the other models are performing in the same way in representing the gravity anomalies. However, for the Bouguer gravity anomaly, it is preferable to use the XGM2019e and for free-air gravity anomaly, the EIGEN-6C4 model is the best based on the results from this research. The results of this study are in agreement with many similar studies focused on the assessment of several GGMs in different region areas [48–50]. These studies concluded that XGM2019e_2159 gives the best fit results for geoid undulation and gravity anomalies values.

6 Conclusion

This study presents an evaluation of the accuracy of several recent and popular GGMs; XGM2016, XGM2019e_2159, EIGEN-6C4, GO_CONS_GCF_2_TIM_R6e, and EGM2008 using actual GNSS/leveling and terrestrial gravity dataset to identify the best model that fits the study areas which are located along the Mediterranean Sea and Red Sea coastal lines in Egypt. The selection of these areas was due to their continuous need for protection works to fight against the coastal erosion caused by climate change and global warming. And also, there are many important urban, tourism, and development projects that are being held continuously along these areas So, it is necessary to have an accurate geoid model to estimate the orthometric heights with an acceptable accuracy and also to have a suitable gravimetric model to conduct geodynamic and geophysical explorations as crustal movements. Based on the obtained results and statistics, following conclusions were drawn:

A general consistency in all five under investigation GGMs data is observed in both the undulation variations and gravity anomalies data. Regarding the geoid undulation results, GO_CONS_GCF_2_TIM_R6e model is the best fit GGM for the estimation of geoid model in region A, along the Mediterranean Sea, while XGM2019e_2159 model is the best suitable for region B, along the Red Sea. It should be noted that according to the results obtained from this study, the investigated GGMs cannot replace the leveling works specially engineering works which requires high accuracy.

Regarding the gravity anomalies estimated results, all investigated GGMs except GO_CONS_GCF_2_TIM_R6e model perform in the same way in representing the gravity anomalies, Bouguer and free-air. XGM2019e_2159 model is the best fit GGM for determination of Bouguer gravity anomaly and EIGEN-6C4 model is the best for free-air gravity anomaly.

Due to the data contribution from recent Earth gravity field satellite missions and other data sources, GGMs have been advanced dramatically. However, this progress is limited by the suitability of using such models to represent certain area in terms of accuracy and applications. The value of RMSE of the undulation variation obtained in this study (0.669 m for zone A and 0.303 m for zone B) may help in some civil engineering applications that meet this accuracy level. Regarding the gravity anomalies, several GGMs might be reliable for different zones area. Therefore, for this study area, the most reliable GGMs is XGM2019e_2159 and EIGEN-6C4 for Bouguer and free-air gravity anomaly modeling, respectively.

Acknowledgements: The authors are grateful to the Bureau Gravimetrique International (BGI) and to the International Center for Global Earth Models (ICGEM) for their help in providing data used in this study.

Funding information: This research work was funded by Institutional Fund Projects under Grant No. IFPIP-1333-137-1443. The authors gratefully acknowledge the technical and financial support provided by the Ministry of Education and King Abdulaziz University, DSR, Jeddah, Saudi Arabia.

Author contributions: Ahmed Alshouny: contributed to all aspects of this work. Ragab Khalil and Abdullah Kamel: validation, analysis, and writing – review and editing. Yehia Miky: investigation, validation, formal

analysis, and writing – review and editing. All authors have read and agreed to the published version of the manuscript.

Conflict of interest: Authors state no conflict of interest.

Data availability statement: Data used in this study can be obtained from the corresponding author on reasonable request.

References

[1] El Shouny A, Nagy Y. Comparative study of different surface fitting methods for geoid modeling along the Rosetta Coastal Zone Area. Sharm El-Sheikh, Egypt: Regional Conference on Surveying & Development; 2015. p. 3–6.

[2] Zaki A. Assessment of GOCE Models in Egypt. PhD thesis. Egypt: Faculty of Engineering at Cairo University; 2015.

[3] Gad MA, Odalović OR, Zaky KM. Tailoring a global harmonic model XGM 2016 to the territory of Egypt. Int J Sci Eng Res. 2018;9:1–5.

[4] El Shouny A, Al-Karagy EM, Mohamed HF, Dawod GM. Gis-based accuracy assessment of global geopotential models: A case study of Egypt. Am J Geographic Inf Syst. 2018;7:118–24. doi: 10.5923/j.ajgis.20180704.03

[5] Awwad TM. Investigation the accuracy of different global geopotential models data over Egypt. Int J Sci Eng Res. 2019;10:1470–4.

[6] ABD-Elmotaal HA. Egyptian geoid using ultra-high-degree tailored geopotential model. In Proceedings of the 25th International Federation of Surveyors FIG Congress. Kuala Lumpur, Malaysia: FIG Congress 2014; 2014. p. 16–21.

[7] Awwad TM. Deriving a geoid undulation network over Egypt by merging data of different global geo-potential models. Aust J Basic Appl Sci. 2019;13(7):55–63. doi: 10.22587/ajbas.2019.13.7.9.

[8] Ruby A. Enhancement of global geopotential harmonic models for Egypt. PhD thesis. Egypt: Benha University; 2018.

[9] El Shouny A, Yakoub N, Hosny M. Evaluating the performance of using PPK-GPS technique in producing topographic contour map. Mar Geodesy. 2017;40:224–38. doi: 10.1080/01490419.2017.1321594.

[10] Kamil EA, Takaijudin H, Hashim AM. Mangroves as coastal bio-shield: A review of mangroves performance in wave attenuation. Civ Eng J (Iran). 2021;7:1964–81. doi: 10.28991/cej-2021-03091772.

[11] Rodríguez-Martín J, Cruz-Pérez N, Santamarta JC. Maritime climate in the canary islands and its implications for the construction of coastal infrastructures. Civ Eng J (Iran). 2022;8:24–32. doi: 10.28991/CEJ-2022-08-01-02.

[12] Ramadhan R, Marzuki, Harmadi. Vertical characteristics of raindrops size distribution over Sumatra region from global precipitation measurement observation. Emerg Sci J. 2021;5:257–68. doi: 10.28991/esj-2021-01274.

[13] Hofmann-Wellenhof B, Moritz H. Physical Geodesy. New York: Springer; 2005. ISBN 9783211235843.

[14] Perdana A, Heliani L. Evaluation of Global Geopotential Model and Digital Terrain Model to the Accuration of Local Geoid Model. 7th Annual Engineering Seminar (InAES); 2017.

[15] Borghi A, Barzaghi R, Al-Bayari O, Al Madani S. Centimeter Precision Geoid Model for Jeddah Region (Saudi Arabia). Remote Sens (Basel). 2020;12:2066. doi: 10.3390/RS12122066.

[16] Ince ES, Barthelmes F, Reißland S, Elger K, Förste C. ICGEM – 15 years of successful collection and distribution of global gravitational models, associated services, and future plans. 2019;59:647–74.

[17] ICGEM International Center for Global Gravity Field Models http://icgem.gfz-potsdam.de/home (accessed on 17 April 2020).

[18] Aman S, Sulaiman H, Talib KH, Wazir MA, Yusof OM. Evaluation of Geoid Height Derived by Geopotential Model and Existing Regional Geoid Model. 2013 IEEE 9th International Colloquium on Signal Processing and its Applications; 2013. p. 106–10. doi: 10.1109/CSPA.2013.6530024.

[19] Aman S, Sulaiman H, Naim N, Talib KH, Wazir MA, Yusof OM. Deriving Orthometric Height Using Global Geopotential Models (GGMs). 7th IEEE Control and System Graduate Research Colloquium (ICSGRC); 2016. p. 193–6. doi: 10.1109/ICSGRC.2016.7813326.

[20] Erol B, Sideris MG, Çelik RN. Comparison of Global Geopotential Models from the CHAMP and GRACE missions for Regional Geoid Modelling in Turkey. Studia Geophysica et Geodaetica. 2009;53:419–41.

[21] Barthelmes F. Global Models. In Encycl Geodesy. Cham: Springer International Publishing; 2014. p. 1–9.

[22] Amos MJ, Featherstone WE. Comparisons of recent global geopotential models with terrestrial gravity field observations over New Zealand and Australia. Geomat Res Australas. 2003;79:1–20.

[23] Botai CM, Combrinck L. Global geopotential models from satellite laser ranging data with geophysical applications: A review. South Afr J Sci. 2012;108:1–10.

[24] Wu Q, Wang H, Wang B, Chen S, Li H. Performance comparison of geoid refinement between XGM2016 and EGM2008 based on the KTH and RCR methods: Jilin Province, China. Remote Sens. 2020;12:324.

[25] Heck B. An evaluation of some systematic error sources affecting terrestrial gravity anomalies. Bull Géodésique. 1990;64:88–108. doi: 10.1007/BF02530617.

[26] Zingerle P. Short note: The experimental geopotential model XGM2016. J Geod. 2018;92:443–51. doi: 10.1007/s00190-017-1070-6.

[27] Förste C, Bruinsma S, Abrikosov O, Flechtner F, Marty J-C, Lemoine J-M, et al. EIGEN-6C4-The Latest Combined Global Gravity Field Model Including GOCE Data up to Degree and Order 1949 of GFZ Potsdam and GRGS Toulouse. Vol. 16; 2014.

[28] Kim KB, Yun HS, Choi HJ. Accuracy evaluation of geoid heights in the national control points of South Korea using high-degree geopotential model. Appl Sci. 2020;96:1466.

[29] Brockmann JM, Schubert T, Mayer-Gürr T, Schuh WD. The Earth's Gravity Field as Seen by the GOCE Satellite - an Improved Sixth Release Derived with the Time-Wise Approach (GO_CONS_GCF_2_TIM_R6). GFZ Data Services; 2019.

[30] Forsberg R, Olesen AV, Ferraccioli F, Jordan T, Corr H. PolarGap 2015/16; 2017.
[31] Scheinert M, Ferraccioli F, Schwabe J, Bell R, Studinger M, Damaske D, et al. New antarctic gravity anomaly grid for enhanced geodetic and geophysical studies in Antarctica. Geophys Res Lett. 2016;43:600–10. doi: 10.1002/2015GL067439.
[32] Forsberg R, Skourup H, Andersen OB, Knudsen P, Laxon SW, Ridout A, et al. Combination of Spaceborne, Airborne and *In Situ* Gravity Measurements in Support of Arctic Sea Ice Thickness Mapping; 2007.
[33] Zingerle P, Brockmann JM, Pail R, Gruber T, Willberg M. The polar extended gravity field model TIM_R6e. GFZ Data Services; 2019.
[34] Pavlis KN. An Earth Gravitational Model to Degree 2160: EGM2008. The 2008 General Assembly of the European Geosciences Union. Vienna, Austria; April 13–18, 2008.
[35] Fecher T, Pail R, Gruber T. GOCO05c: A new combined gravity field model based on full normal equations and regionally varying weighting. Surv Geophys. 2017;38:571–90. doi: 10.1007/s10712-016-9406-y.
[36] Pail R, Fecher T, Barnes D, Factor JF, Holmes SA, Gruber T, et al. Short note: The experimental geopotential model XGM2016. J Geod. 2018;92:443–51. doi: 10.1007/s00190-017-1070-6.
[37] Zingerle P, Pail R, Gruber T, Oikonomidou X. The Experimental Gravity Field Model XGM2019e. GFZ Data Services; 2019. doi: 10.5880/ICGEM.2019.007.
[38] Sinem Ince E, Barthelmes F, Reißland S, Elger K, Förste C, Flechtner F, et al. ICGEM – 15 years of successful collection and distribution of global gravitational models, associated services, and future plans. Earth Syst Sci Data. 2019;11:647–74. doi: 10.5194/essd-11-647-2019.
[39] Erol B, Isık MS, Erol S. An assessment of the GOCE high-level processing facility (HPF) released global geopotential models with regional test results in Turkey. Remote Sens. 2020;12:586.
[40] Yilmaz M, Yilmaz I, Uysal M. The evaluation of gravity anomalies based on global models by land gravity data. 2018;12:829–35.
[41] Hill P, Bankey V, Langenheim V. Introduction to potential fields: Gravity. USGS Fact Sheet. 1997;239:1–2. doi: 10.1144/GSL.SP.1997.123.01.01.
[42] Yılmaz M, Kozlu B. The comparison of gravity anomalies based on recent high-degree global models. Güncel Yüksek Dereceli Küresel Model Temelli Gravite Anomalilerinin Karşılaştırılması. 2018;18:981–90.
[43] Survey Research Institute (SRI) Technical Report of the Survey Work Performed along Egyptian Coastal Zone Areas as a Part of the Project "Establishment and Strengthening Surveying Benchmarks along Egyptian Coast Using GPS and Levelling Measurements." 2014.
[44] Adm R, Bossler JD. Standards and specifications for geodetic control networks. Rockville, Maryland: Federal Geodetic Control Committee; 1984.
[45] Doma MI, El Shoney AF. A new method for designing the optimum geodetic networks using genetic algorithms. J Eng Appl Sci. 2011;58:109–25.
[46] Land Gravity Data/Gravity Databases/Data/Products/BGI - BGI Available online: http://bgi.omp.obs-mip.fr/data-products/Gravity-Databases/Land-Gravity-data (accessed on 17 April 2020).
[47] Morelli C, Gantar C, Honkasalo T, McConnel RK, Tanner JG, Szabo B, et al. The International Gravity Standardisation Net 1971 (IGSN71). Special Publication No. 4; 1974.
[48] Lee J, Kwon JH. Precision evaluation of recent global geopotential models based on GNSS/leveling data on unified control points. J Korean Soc Surv Geodesy Photogramm Cartogr. 2020;38(2):153–63.
[49] Osman ASM, Anjasmara IM, Ruby A, Udama ZA. Assessment of high-degree reference models and Recent Goce/Grace Global Geopotential Models over Sudan based on the GPS/Leveling data. In IOP Conference Series: Earth and Environmental Science; 2021, December. Vol. 936, Issue 1. p. 012035. IOP Publishing.
[50] Hussen MM. Evaluation of Global Gravity Field Models using GPS and Leveling Data over Ethiopia. MSc thesis. Ethiopia: Addis Ababa University; 2021.